ISSN 1330-3651(Print), ISSN 1848-6339 (Online)
UDC/UDK 004.942:627.13

THE NUMERICAL MODELLING OF SUSPENDED SEDIMENT PROPAGATION IN SMALL TORRENTS WITH THE APPLICATION OF THE CONTACT DYNAMICS METHOD

Elvis Žic, Nenad Bićanić, Tomasz Koziara, Nevenka Ožanić

Original scientific paper
This paper describes the SOLFEC computational code used to simulate multi-body systems with constraints. The code implements an instance of the Contact Dynamics (CD) method by Moreau and Jean, therefore the constraints are handled implicitly. One of the main goals of the software is to provide a user-friendly platform for testing formulations and solution methods for the (dynamical) frictional contact problem. This paper also describes a method used to develop a computer code written in the Python programming language that is needed to produce a numerical model of suspended sediment propagation. The paper also provides graphical representations of the Mud Flow simulation in the hypothetical example inside of the Salt Creek stream erosional base in Croatia.

Keywords: *Contact Dynamics method, numerical modelling, Salt Creek stream, SOLFEC program, suspended material*

Numeričko modeliranje propagacije suspendiranog nanosa na malim vodotocima primjenom metode dinamike kontakta

Izvorni znanstveni članak
U radu je opisan SOLFEC program za izvršavanje dinamike (simulacije) sustava kontakata više tijela s ograničenjima. Solfec računalni kod provodi dinamiku kontakata prema metodi Moreaua i Jeana, pa se stoga sa ograničenjima rukuje implicitno. Jedan od glavnih ciljeva programa je osigurati korisniku platformu za ispitivanje formulacija i rješenja za dinamičke metode problema kontakata putem trenja. U radu je opisana i metoda kreiranja računalnog koda pisanog u Python programskom jeziku potrebnog za izradu numeričkog modela propagacije suspendiranog nanosa. Dani su grafički prikazi simulacije tečenja suspendiranog nanosa na hipotetskom primjeru erozijske baze vodotoka Slani potok (Hrvatska).

Ključne riječi*: metoda dinamike kontakata, numeričko modeliranje, Slani potok, SOLFEC program, suspendirani materijal*

1 Introduction

An unbound rock material analysis is important for assessing risk and delimitating vulnerable areas where mitigation measures are required. A numerical model is the most accurate and efficient tool for debris flow and mud flow analyses.

Debris flows travel at an extremely rapid velocity and can impact large areas that are often far from their source. In mountain valleys, settled areas are generally situated close to torrents or rivers because these areas are more favourable to urban development [1]. Therefore, these areas are located where sediments and debris are deposited from the channel. The prediction of debris flow propagation (including the deposition area and the impact within it) is called a "run out analysis" [2]. This analysis can provide relevant information for land use planning. These methods must be quantitative and as accurate, objective and accessible as possible. Debris flow models should easily give flow velocity, flow depth, discharge and debris volume as outputs. Moreover, models should require few adjustable input parameters. There are currently several numerical programs and mathematical codes used in unbound rock material analysis, including the SPH model (Smoothed Particle Hydrodynamics model), PFC^{3D} code (Particle Flow Code in 3D), SOLFEC numerical program, FLO2D and MIKE 11.

2 Unbound suspended rock material flow

This paper provides a brief description of the creation and execution of commands within the SOLFEC program used to simulate the flow of unbound suspended rock material. Debris flows (*DF*) are a type of mass wasting process. Mass movement processes can be categorized by certain parameters, such as the release mechanism, material type, sediment composition, proportion of the solid phase, velocity, time of the event, slope of the movement plane, material behaviour, and the physical processes that occur during the mass movement. Currently, one of the most accepted classifications is that of Hungr et al. (2001, 2005) [3]. Using this classification and the definitions given by Stiny (1910) and Sharpe (1938), debris flow can be defined as an extremely rapid flow in a steep, confined channel that is deposited on a debris fan. Debris flow occurs after a flood, and it is a viscous mass (non-Newtonian fluid) consisting of water, soil, gravel, rocks and woods. Mudflows (*MFs*) can be defined as a fine-grained debris flow. If it derives from volcanic sources, it is called a "lahar" [1, 2].

Debris is made up of loose, unsorted material of low plasticity, such as that produced by mass wasting processes, weathering, glacier transport, explosive volcanoes and human activity (e.g., mine debris). Debris is a mixture of sand, gravel, cobbles, and boulders and can contain organic material (e.g., logs, tree stumps, tree trunks). The consistency of debris is non-plastic or weakly plastic. Mud is defined as a soft, remoulded clayey soil with a significantly plastic matrix (sand or finer) and liquidity index during motion of greater than 0,5 [1].

Debris flows are composed of water and debris (solid particles). The solid phase occupies a larger volume than the liquid phase [4]. The solid particles can be classified into fine particles (clay, silt and sand) and coarse particles (gravel, cobbles, boulders and organic particles). Debris flows and mudflows have similar water concentrations, but they have different solid particle sizes. Boulders can have diameters as large as a few meters. Boulders

typically look suspended in the mass; therefore, it is difficult to estimate them during the course of motion.

Debris flow, like other gravitational mass movements, can be divided into several phases: the initiation phase, in which the initial mass is released; the transition phase, in which the initial mass propagates along the travel path; and the deposition phase, in which the mass stops and is deposited on a colluvial fan [5] (Fig. 1).

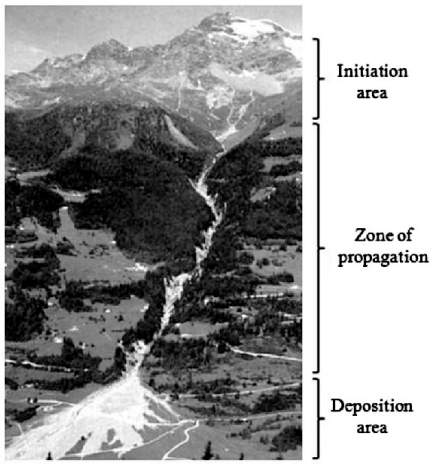

Figure 1 Debris flow of Val Varuna (1987) [5]

Debris flows are unsteady and non-uniform because they move downslope as waves or series of waves [6]. They are pulsating flows in which surges are separated by a watery intersurge flow. Surges can become sporadic due to flow instability, the occurrence of consecutive landslides that release material, or a slowdown of the flow followed by a boulder dam break. The volume of each surge may vary, and the time in between surges ranges from seconds to hours. Debris flow events can be composed of one to many tens of waves. For instance, the Val Varuna debris flow, which occurred on the 18th of July in 1987, was a succession of approximately 10 surges. The volume of the debris flow was 200 000 m^3, and the maximum volume per surge was 50 000 m^3 [5].

Debris flows are typically mobilized from either numerous small landslides or one large landslide. They occur when a debris slide or landslide changes into a debris flow [7]. Mobilization is the process of forming debris flows from a static mass of water-laden soil, sediment or rock. Mobilization occurs under the following three conditions: the failure of the mass, a sufficient amount of water to saturate the mass and a sufficient conversion of gravitational potential energy to internal kinetic energy. The conversion of the energy changes the type of mass movement from a slide on a failure surface to a flow [2, 3, 7].

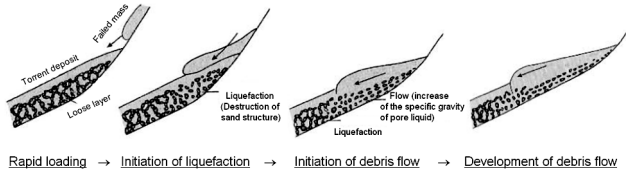

Figure 2 Illustration of the initiation of debris flow (Sassa, 1985) [8]

In addition to the water content in the soil, torrents can also increase the water content. However, the required amount of water is typically already contained in the soil mass when the failure occurs. In this case, the water comes from rainfall infiltration. When the initial landslide mass rides on the torrent bed deposits (Fig. 2), an undrained loading process may generate a high pore-water pressure within the torrent deposits. This high pore-water pressure helps incorporate those deposits into a moving mass.

This phenomenon, which results in the entrainment of the bed material, is called the liquefaction failure of the torrent deposits and causes the volume of the debris flow to increase significantly. Debris flow can also initiate from channel bed and bank erosion. A sufficient water discharge is required to start the erosion process. The flow rapidly erodes the bed and mixes a large solid volume with the water. It sets off an irreversible chain of reactions, which increases the solid concentration of the mixture. The required conditions for the formation of debris flow are channel bed and bank erosion capacity, water discharge and slope (Fig. 3).

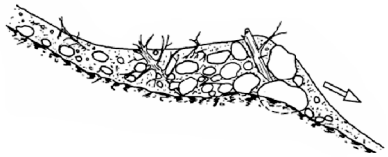

Figure 3 Natural dam composed of organic and soil debris [9]

3 Debris flow modelling on the Salt Creek stream

In the Croatian-Japanese research project entitled "Project on Risk Identification and Land-Use Planning for Disaster Mitigation of Landslide and Floods in Croatia", a group of scientists from the Faculty of Civil Engineering University of Rijeka (Flash-flood and Debris Flow Working Group, WG2) carried out systematic observations of the meteorological and hydrological parameters of the Salt Creek stream's catchment area in real time using ombrografs, water level instruments, satellite radar, flow meters (based on the Doppler effect) and piezometers (to monitor groundwater levels).

These data were collected to conduct numerical and hydrological analyses of the measured parameters and to develop simulation models of floods, mudflows and flow, which can provide early warnings of floods and torrential phenomena burglary and evaluate the rates at which they coincide with landslides.

After the meteorological and hydrological data were collected, the next research step was to develop mathematical and physical models for the various scenarios of moving floodwater waves and movement of soil and stone material with water along the Salt Creek stream.

The equipment used to make the meteorological and hydrological observations was largely donated by the Japanese Government for the analysis of selected exploration areas around the city of Rijeka. The Faculty of Civil Engineering University of Rijeka also provided some equipment. Systematic monitoring in real time of the analysed area will be established based on the results of this research supplemented with new research and results analysis. In addition to recently collected data, the historical time series of meteorological and hydrological

data obtained from relevant authorities will also be used. In the laboratory investigations, physical models will be developed, and flow simulations of different flood and mudflow scenarios will be performed.

3.1 Description of the Salt Creek catchment area

The Salt Creek stream is located in the Dubračina River catchment area, located in Primorsko-Goranska County in the hinterland of the Crikvenica city, which extends from the northwest to southeast, parallel to the Adriatic coast (Fig. 4). The Dubračina River extends from Križišće village to the northwest and Novi Vinodolski to the southeast and the River's Vinodol channel extends to coastal areas.

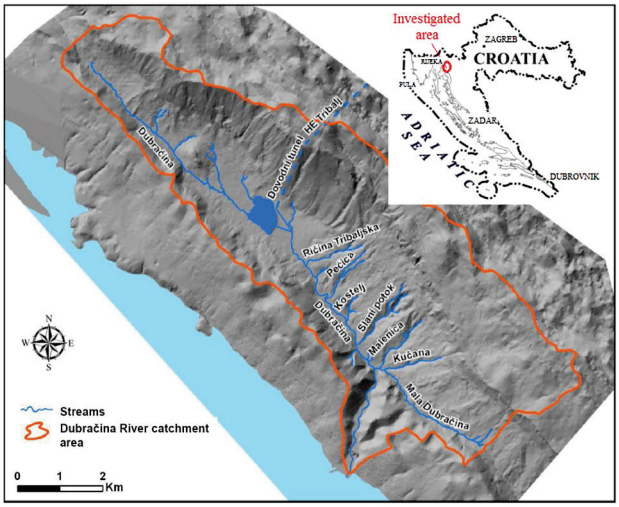

Figure 4 Hydrographic network in the Dubračina River catchment area [10]

The Dubračina River catchment area is 43,5 km^2 (forest and semi-natural areas are 38 km^2, agricultural land is 3 km^2, and built-up areas (roads and buildings) are 2 km^2). There is intense erosion in the Dubračina River catchment area, particularly on the slopes of the Salt Creek stream, where the so-called landscape type "badlands" has formed [11]. Numerous active and calmed landslides, together with erosion, represent the dominant geomorphic processes and major geological hazards. Altitude in the Dubračina catchment area varies from 5-920 m.a.s.l., with the dominant slope of the mountain (58 %) ranging from 5° to 20°. The Dubračina River Valley in the northeast is surrounded by steep cliffs up to 920 m.a.s.l. The cross-section of the Dubračina basin is asymmetric, with a longer northeastern slope and shorter western slope. The highest point on the southwest side of the basin is 357 m.a.s.l., while the bottom of the valley is 30 m.a.s.l. [11, 12]. The Dubračina River basin was an isolated geographic unit of the eastern area of Kvarner. The riverbed of Dubračina River is mainly located on the coastal ridge [11]. The karst carbonate rocks (mainly Upper Cretaceous and Paleogene limestone) are represented on the slopes of the peak areas of the basin and cover 55 % of basin area. Limestone cliffs located at the northeastern edge of the basin represent the edge of the karst plateau.

The central and hypsonometric lower parts of the Dubračina basin are characterized as scrolling within the slope sediments, composed of a mixture of particulate clay with fragments of sandstone and limestone. Instable slopes in the Dubračina basin are caused by geomorphological processes (fluvial erosion in the foot of the slope) and physical processes (intensive short-term rainfall). Precipitation (and potentially an earthquake) is the most common initiator of the slip. In the Dubračina River basin, there are important small and shallow slip surface sediments (rock creep and debris) on the boundary with fresh rock mass. The landslides caused significant economic losses due to continuous damage to roads, infrastructure, houses and bed surface flows [13, 14].

The Salt Creek catchment area, which is approximately 2 km^2, is located at altitudes ranging from 50 to 700 m.a.s.l. (Fig. 5).

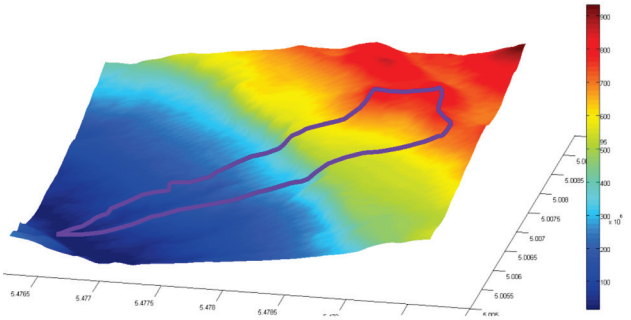

Figure 5 Map of the slopes in the Salt Creek catchment area [15]

The lower part of the catchment area (0,9 km^2) is covered with flysch and produces most of the surface runoff. The upper part of the basin is mostly rocky ledge and produces a negligible amount of surface runoff. In the contact zone of karst and flysch, there are many overflow sources that make up the bulk of water balance in the dry season (Fig. 6). The affected surface of the erosion base is approximately 3 km^2, so they compromise the surrounding settlements in Belgrad, Baretići, Grižane and Kamenjak, as well as the surrounding roads (Fig. 6).

a) b)

Figure 6 a) Salt Creek stream (winter period), b) erosion base of the Salt Creek stream (Photo: Elvis Žic)

The retentions are almost completely filled with sediment (mostly silt). Despite numerous rehabilitation measures implemented during the 20th century, there is still a general degradation of the terrain and thus properties of a "permanent disaster" [13]. The middle slope of the basin is 22 %, the slopes range from 5 % to 100 % (Fig. 5), which means the basin is very steep. The slopes of the catchment area determine the runoff and erosion processes. The time concentration of the basin by Kirpich is 15 minutes [15]. If part of the flysch basin is considered, the middle slope is 19 %, and the concentration time is 9 minutes.

3.2 Digital elevation model of the Salt Creek erosional base

A digital orthophoto of the Salt Creek area was made at a scale of 1:5000, as shown in Fig. 7. By combining the orthophoto in AutoCAD with a frame, network mapping and an external description, a digital orthophoto map was created. To further emphasize the configuration of the terrain, contours and dimensions were drawn on the orthomap. In this manner, a georeferenced basis was obtained in a digital format that can be compared with the development of the Croatian-Japanese research project. A more accurate reconstruction can be obtained by supplementing the data from the terrain and drawing and redrawing the position of measuring instruments based on a variety of analyses to obtain the closest ideal reconstruction.

The digital orthophoto, which can be used separately or in association with vector data, can be used to obtain simple information, such as coordinates of points, distances, areas and volumes. The orthophoto was projected on a digital elevation model (DEM) using a photorealistic terrain model. The DEM corresponds to the actual look of the Salt Creek area (Fig. 8). The digital elevation models of the Dubračina River (Fig. 8) and Salt Creek stream (Fig. 9) are numerically defined by a series of points with three coordinates (X, Y and Z) in digital form. Unlike the Digital Terrain Model (DTM), which includes vegetation, buildings, and fracture lines to better approximate the terrain, this model does not contain vegetation or constructed structures.

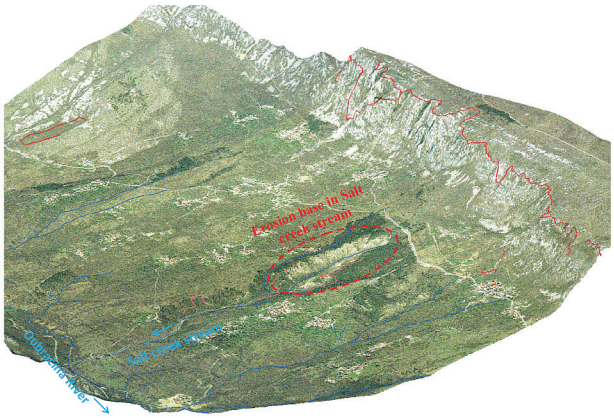

Figure 7 Orthophoto image "coated" over the Digital Terrain Model [15]

Points in the DEM were obtained by direct surveys of the terrain, photogrammetric surveys, satellite data georeferencing, and map digitization (with points and contour lines). The result of the Digital Terrain Model can be shown with three-dimensional lines (with lines and turning points), striking individual points (elevations), contour lines and elevations (Digital Height Model - DHM), profiles and relief shading [16].

Based on the DEM of the Dubračina River basin, we created the GIS database for the Salt Creek stream. In addition to collecting and entering spatial data, the attribute data that was collected from gauges, accurate meteorological stations, diver instruments for measuring the surface and groundwater levels, radar devices, ombrografs and other measuring devices installed in the same area were also imported into the GIS database.

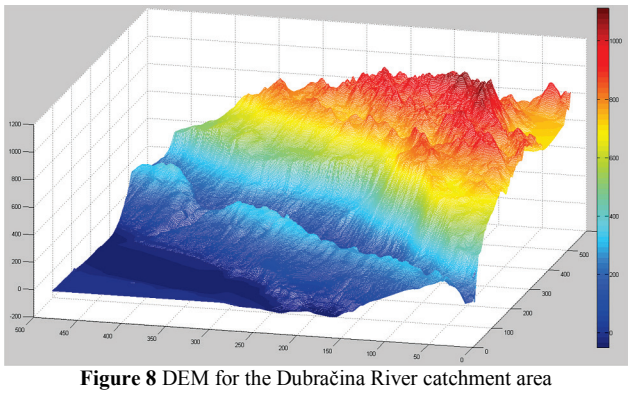

Figure 8 DEM for the Dubračina River catchment area

Currently, collected geometric data can be displayed in vector or raster form. Data in vector format describes spatial objects using set point coordinates in a coordinate system. The vector form of GIS is more complex (because it uses very complex spatial operations) and is more precise than the raster form of GIS [16].

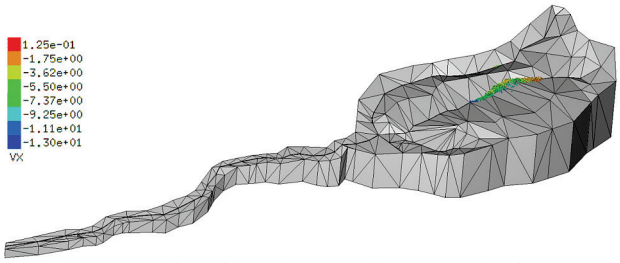

Figure 9 DEM of the Salt Creek erosional base created in the SOLFEC program

Vector data can be edited and changed easily to correspond with graphical and descriptive data. Raster data in GIS are shown as a surface that consists of dots and looks like a polygonal mesh of different shapes and sizes [16]. The vector and raster data models supplemented each other, and today's software support allows for the conversion of one form to another. After entering data into the GIS, the data needs to be edited (to eliminate errors) or processed further.

3.3 Spatial and temporal discretization

The mathematical model for solving debris and mud flows is a system of differential equations. Once the model is set, the resolution on the computer needs to be adjusted (i.e., the appropriate method for discretization of space and time needs to be used within the SOLFEC application). The most important approaches to discretize spaces are the Finite Difference Method (FDM), Finite Volume Method (FVM) and Finite Element Method (FEM). The SOLFEC program uses the FEM to solve the governing equations and discretize the space. This method divides the domain of solutions into a finite number of adjacent control elements arranged in arbitrary triangles, tetrahedra and hexahedra (Fig. 10). The components of the velocity vectors (u on the x coordinate axis, v on the y coordinate axis and w on the z coordinate axis) are defined in the centres of each element. The other scalar

value is defined in the centre of each element. In addition to selecting the appropriate type of numerical mesh, an approximation that will be used in the discretization process needs to be chosen. In the FEM, it is necessary to choose the shape functions (elements) and their weight functions. When selecting the shape functions, the simplicity, ease of implementation, accuracy and computational efficiency of the options must be considered.

In the FEM implemented in the SOLFEC program, the domain is broken up into a set of discrete volumes or finite elements, which are generally unstructured (two-dimensional spaces are typically triangles or quadrangles, while three-dimensional spaces are tetrahedra or hexahedra). In this method, the equations are multiplied with a weighting function before the entire domain is integrated. In its simplest form, the solution is represented by a linear function for each element, guaranteeing the continuity of solutions at the boundaries of the element. Weighting functions are typically in the same form.

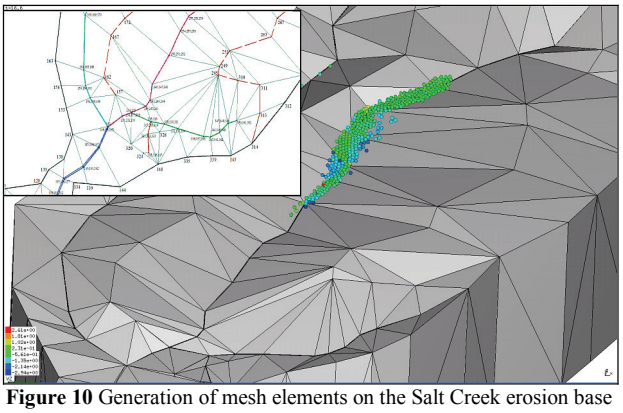

Figure 10 Generation of mesh elements on the Salt Creek erosion base

When unstable flows are computed, time (the fourth dimension) must be taken into account; time, as well as space, must be discretized. The direction of influence is the main difference between the temporal and spatial coordinates. For example, the force in any spatial location can affect the flow motion elsewhere, while the use of force at a given time can only affect future flows (no backward influence). After the spatial derivatives in the main equations are discretized (i.e., the Navier-Stokes or Euler equations for flow), the associated system of nonlinear differential equations shown below is obtained.

$$\frac{\mathrm{d}\vec{u}}{\mathrm{d}t} = \vec{F}(\vec{u},t). \tag{1}$$

This equation can be integrated in time using a method for solving the unstable flow problem. All methods of computation are advanced through time step-by-step, or "marching" (time-marching methods), to meet the weather conditions [17]. To solve the steady flow, spatial discretization leads to the connected system of nonlinear algebraic equations

$$\vec{F}(\vec{u}) = 0. \tag{2}$$

Some iterative methods need to be introduced to solve the nonlinearity of above equations and thus obtain the solutions.

3.4 Numerical code and simulation

To carry out simulations in the SOLFEC program, previously printed numeric code needs to be implemented using the Python programming language. SOLFEC is a computational code used to simulate multi-body systems with constraints. Because the SOLFEC code implements an instance of the Contact Dynamics (CD) method by Moreau and Jean [18, 19], the constraints are handled implicitly. One of the main goals of the software is to provide a user-friendly platform for testing formulations and solution methods for the (dynamic) frictional contact problem. It also serves as a development platform for other aspects of time-stepping methods (e.g., contact detection, time integration). The code implements several kinematic models (rigid, pseudo-rigid, finite element), contact detection algorithms, time integrators and constraint solvers (e.g., penalty, Gauss-Seidel) [20, 21].

Each source code in the SOLFEC program can be upgraded with the aforementioned structures and routines. As an object-oriented language, Python makes it easy to write a scripting language in the SOLFEC program. Python code was executed by scripting, which saves the code within a text file that is executed when the program starts. One or more algorithmic steps often need to be repeatedly executed (with the help of algorithmic loop) within the Python code; these repeat executions may change the default data processing. Such repetition is performed until a set condition is fulfilled or unfulfilled. The input file that specifies the geometry of the terrain (generating mesh using finite elements) can be connected with defined commands in the Python code.

Some basic concepts are introduced to provide a greater understanding of the SOLFEC computer code. First, suppose that there are four different bodies, as shown in Fig. 11.

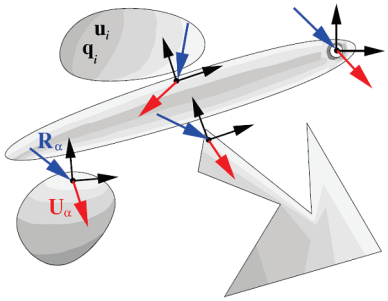

Figure 11 Four different bodies for the SOLFEC program application

The placement and velocity of each point in every body are determined by a configuration q_i and velocity u_i, respectively. Let q and u collect the configurations and velocities of each of the bodies. If the time history of velocity is known, the configuration time history can be computed as

$$q(t) = q(0) + \int_0^t u \,\mathrm{d}t. \tag{3}$$

The velocity is determined by integrating Newton's law

$$u(t) = u(0) + M^{-1}\int_0^t \left(f + H^{\mathrm{T}}R\right)\mathrm{d}t, \tag{4}$$

where M is an inertia operator (assumed as constant here), f is an out-of-balance force, H is a linear operator, and R collects some point forces R_α. A number of local coordinate systems (local frames) are monitored while integrating the motions of the bodies. There are four local frames in Fig. 11, each of which is related to a pair of points that typically belong to two distinct bodies. An observer embedded in a local frame calculates the local relative velocity u_α of one of the points as viewed from the perspective of the other point [20]. Let U collect all of the local velocities. Then, a linear transformation H can be found, such that

$$U = Hu. \tag{5}$$

In this case, local frames correspond to constraints. The local relative velocities are influenced by applying local forces R_α. This can be collectively described by the implicit relationship

$$C(U,R) = 0. \tag{6}$$

The implicit relationship shown in Eq. (6) must be solved at each moment of time to integrate Eqs. (3) and (4). An example of a numerical approximation of such a procedure is shown below:

$$q^{t+\frac{h}{2}} = q^t + \frac{h}{2}u^t, \tag{7}$$

$$u^{t+h} = u^t + M^{-1}hf^{t+\frac{h}{2}} + M^{-1}H^{\mathrm{T}}R, \tag{8}$$

$$q^{t+h} = q^{t+\frac{h}{2}} + \frac{h}{2}u^{t+h}, \tag{9}$$

where h is a discrete time step. Because the time step h does not appear by $M^{-1}H^{\mathrm{T}}R$, R should be interpreted as an impulse (an integral of reactions over $[t,\ t+h]$). At the beginning of the procedure q^0 and u^0 as prescribed initial conditions. The out-of-balance force

$$f^{t+\frac{h}{2}} = f\left(q^{t+\frac{h}{2}}, t+\frac{h}{2}\right), \tag{10}$$

incorporates both the internal and external forces. The symmetric and positive-definite inertia operator

$$M = M\left(q^0\right), \tag{11}$$

is computed once during the procedure, while the linear operator

$$H = H\left(q^{t+\frac{h}{2}}\right), \tag{12}$$

is computed at every time step. The number of rows in H depends on the number of constraints, while its rank is related to their linear independence. We then compute B and W using

$$B = H\left(u^t + M^{-1}hf^{t+\frac{h}{2}}\right), \tag{13}$$

and

$$W = HM^{-1}H^t, \tag{14}$$

which are symmetric and semi-positive definite. The linear transformation

$$U = B + WR, \tag{15}$$

maps the constraint reactions R into local relative velocities ($U=Hu^{t+h}$ at time $t+h$). In this paper, Eq. (15) is referred to as the local dynamics. Finally, R is such that

$$C(U,R) = C(B+WR,R) = C(R) = 0, \tag{16}$$

where C is a nonlinear and typically non-smooth operator.

Individual SOLFEC objects were created to define both the surface material by which the flow propagated and the type of material (shape, size, physical properties, and so on) that will be propagated downstream. When writing numerical code, the input parameters (Young's modulus, Poisson's ratio, friction coefficient, cohesion coefficient, and so on) must be defined such that the contact between the fluid and immobile soil or suspended (unbound) materials due to the flow are precisely described. Selecting the erosion laws (Egashira or Voellmy erosion law) that will ultimately provide a more realistic picture of propagation of the suspended unbound rock material is an important task.

A contact point and normal direction result from an overlap of two convex objects. The point and normal direction derived from an overlap are well defined for non-smooth geometry. The minimum number of contact points should be used while still maintaining the accuracy of the contact resolution by mesh refinement. At this point, all possible volumetric overlaps will be detected by applying the contact detection algorithm. All contact points are examined and compared with other contact points that are adjacent through common bodies [20]. A contact point is removed if its area is smaller than that of a topologically adjacent neighbouring contact point. A contact point is also removed if the two contact points coincide. Topological adjacency of contact points indicates that they have been created between mesh elements that are topologically adjacent.

The Signorini-Coulomb's law is used to define surface material in the SOLFEC program. The velocity Signorini condition reads

$$\overline{U}_N \geq 0 \quad R_N \geq 0, \ \overline{U}_N R_N = 0, \tag{17}$$

where $\overline{U}_N = U_N^{t+h} + \eta \min(0, U_N^t)$ is the velocity restitution coefficient, U_N is the normal relative velocity, and R_N is the normal reaction. Because the normal direction is consistent with the positive gap velocity, (17) states that any violation of the non-penetration results in a reactive force or velocity driving at the penetration-free configuration. The Newton impact law is accounted for due to $\overline{U}_N$. The Coulomb's friction law reads as follows:

$$\begin{cases} \|R_T\| \leq \mu R_N \\ \|R_T\| < \mu R_N \ \Rightarrow U_T = 0 \\ \|R_T\| = \mu R_N \ \Rightarrow \exists_{\lambda \geq 0} U_T = -\lambda R_T \end{cases}. \tag{18}$$

If the friction force is smaller than μR_N, then sticking occurs. Sliding occurs if the friction force is μR_N and has a direction opposite to that of the slip velocity. The two laws can be expressed compactly as $C(U, R)=0$.

A bulk material is assigned to a volume. For this assignment, the Kirchhoff-Saint Venant law is used. This method simply extends the linearly elastic material to the large deformation regime [20, 21, 22] and is suitable for large rotation, small strain problems. The strain energy function ψ of the Kirchhoff-Saint Venant materials reads as follows:

$$\Psi = \frac{1}{4}\left[F^{\mathrm{T}}F - I\right] : C : \left[F^{\mathrm{T}}F - I\right], \tag{19}$$

where

$$C_{ijkl} = \lambda \delta_{ij}\delta_{kl} + \mu\left[\delta_{ik}\delta_{jl} + \delta_{il}\delta_{jk}\right]. \tag{20}$$

In the above equations, λ and μ are the Lamé constants, and δ_{ij} is the Kronecker delta. The Lamé constants can be expressed in terms of the Young's modulus E and Poisson's ratio ν. Shown below is the first Piola stress tensor, which is computed as a gradient of the hyperelastic potential Ψ[20].

$$P = \partial_F \Psi(F), \tag{21}$$

where F is the deformation gradient. An implicit equation $C(R)=0$ is solved at each time step. Ideally, an exact solution is reached at a certain value of R in which $C(R)=0$. In numerical terms, however, this is not possible. For very large problems, especially for problems in which the number of constraints exceeds the degrees of kinematic freedom, obtaining very accurate solutions is difficult and often impractical [20]. In any case, it is useful to have an accuracy measure that has some physical interpretation. $C(R)$ can be formulated in terms of velocity to compute the accuracy constraints, and can be used to estimate the relative amount of spurious energy that arises from an inexact satisfaction of constraints. The denominator corresponds to the kinetic energy of the relative free motion; therefore, $g(R)$ is the ratio of the spurious energy to the nominal amount of the energy available at the constraints. Diagonal blocks, which are always positive definite, are used because the singularity of W makes it impractical or impossible to invert.

$$g(R) = \sum_\alpha \left\langle W_{\alpha\alpha}^{-1} C_\alpha(R), C_\alpha(R) \right\rangle / \sum_\alpha \left\langle W_{\alpha\alpha}^{-1} B_\alpha, B_\alpha \right\rangle. \tag{22}$$

The next step in the numerical code is to define the numerical scheme and iterative methods for solving differential equations. The debris and mud flows (and the similar phenomena) can be described with partial differential equations, which typically cannot be solved analytically. To use numerical solution methods, discretization methods must be used to approximate the differential equations as a system of algebraic equations, which can be solved on the computer. The approximations in the SOLFEC program are applicable to a small domain in space and time, so that numerical solutions give results in discrete locations in space and time. The accuracy of the numerical solutions depends on the quality of the discretization that was used. One of the most used iterative methods in the SOLFEC program is the Gauss-Seidel method, which is a special case of the SOR method (Successive over-relaxation method). This method converges two times faster than the Jacobi method, although there are many effective methods. An improved version of the Gauss-Seidel method was the Successive pre-relaxation method. The Gauss-Seidel iteration method immediately uses the approximation of elements of a single-column matrix solution calculated in the new iteration step to compute approximations of the coordinates that follow. Iterative methods in the SOLFEC program provide good solutions for small Δt. Problems with a large range of time steps (stiff) are the greatest difficulty encountered in solving regular differential equations. Therefore, it is very important to examine the behaviour of some methods for large time steps.

Development of solvers for unilateral dynamics is one of the main driving forces behind SOLFEC. Solvers can be developed through the classical Gauss-Seidel approach of Contact Dynamics or a somewhat modified penalty solver of the Discrete Element Method. The equation of local dynamics (15) in the Gauss-Seidel method is

$$U_\alpha = B_\alpha + \sum_\beta W_{\alpha\beta} R_\beta, \tag{23}$$

where U_α is the relative velocities and R_α is the reactions at constraint points. U_α, R_α and B_α are three vectors, and $W_{\alpha\beta}$ is a 3×3 matrix block. Each constraint equation can be formulated as follows:

$$C_\alpha\left(U_\alpha, R_\alpha\right) = 0, \tag{24}$$

or

$$C_\alpha\left(B_\alpha + \sum_\beta W_{\alpha\beta} R_\beta, R_\alpha\right) = 0. \tag{25}$$

The Gauss-Seidel algorithm is quite simple. Diagonal block problems are solved until the reaction change is sufficiently small. The Gauss-Seidel paradigm corresponds to the fact that the diagonal problem is solved using the most recent off-diagonal reactions [20], which prevents a perfectly parallel implementation. After all, reactions are updated in a sequence. Nevertheless, the need for sequential processing can be relaxed. Perhaps the most scalable Gauss-Seidel approach to date was devised by Adams [23].

The penalty solver in the SOLFEC application is quite straightforward. On each processor, the constraints are split into $Contacts_i$ (the contact constraints) and $Others_i$, (the bilateral constraints). Next, the contacts are updated using the *spring-dashpot* model, and a local Gauss-Seidel solver is used to calculate the reactions of the bilateral constraints. The Gauss-Seidel approach is used for non-contacts because it is fairly fast and avoids issues related to the penalization of bilateral constraints [20]. Using Gauss-Seidel is possible because bilateral constraints migrate together with bodies and are thus local to the processor (except for the rigid link constraint).

Choosing an integration method (i.e., the approximation model of the movement of suspended unbound rock material over time) is of great importance for models that use a set of differential equations. The integration scheme's biggest problem is that, by choosing the maximum time step, the stability and accuracy of the calculation must be taken into account. For stable integration, a small time step is required, so the time steps should not have been restricted at a size much smaller than the error for limiting the space. For this reason, it is necessary to perform many time steps. After writing a numerical code, the simulation is executed based on the defined input parameters.

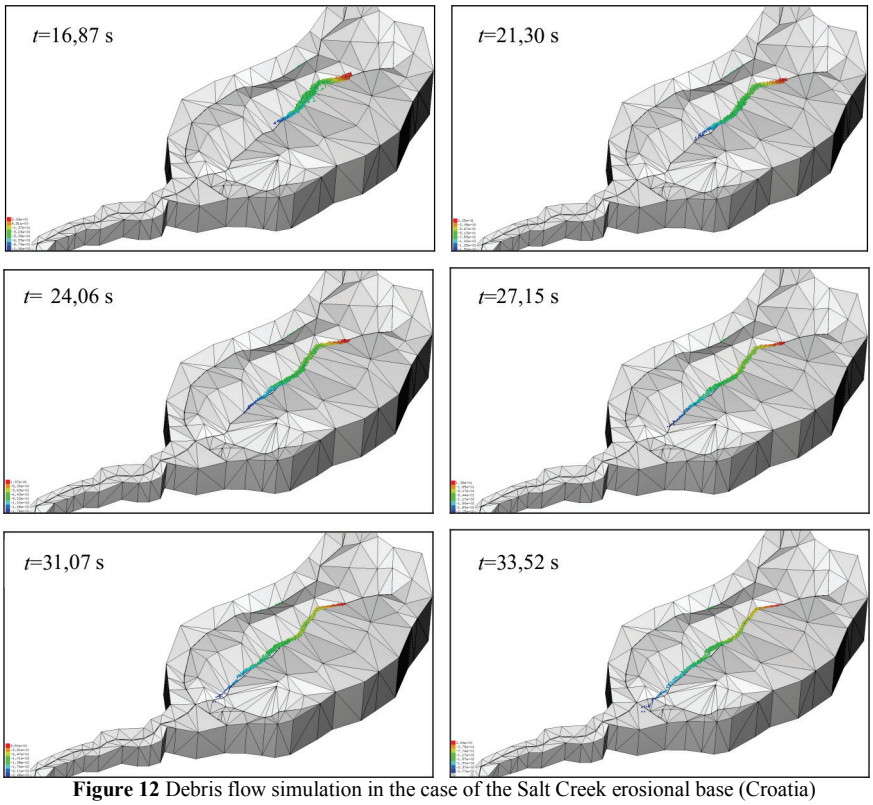

Figure 12 Debris flow simulation in the case of the Salt Creek erosional base (Croatia)

3.5 Simulation and model results

Shown in Fig. 12 and 13 are the simulations for debris flow propagation on the Salt Creek erosional base and deposition of suspended flysch unbound material at the settling tank inside of the Salt Creek stream, respectively.

In these numerical models of flow, a relatively large diameter of the grain material (d=0,3 m, in nature they are large stone pebbles/screens) came into the settling tank because the particles with a small grain diameter (1 mm or less) create a large number of mathematical operations (large number of contact points) when executing the simulation, which requires a lot of memory (i.e., the existence of a cluster (super computer)). Within the simulation in the SOLFEC program, users may view the following derived physical quantities at any time: particle displacements in the x, y and z directions (D_X, D_Y, D_Z, respectively), the velocity of particles (V_X, V_Y and V_Z), the various strains in a particular direction or plane (S_X, S_Y, S_Z, S_{XY}, S_{XZ}, S_{YZ}), forces in contact points, reactions of particles with the surrounding terrain, reaction between the particles, and many other physical quantities (Fig. 14) [24, 25]. In addition, the SOLFEC program can make a detailed list of the simulation data once it is executed (executed entities in time) for each of the required physical quantities [20, 26]. Object *hist = HISTORY (solfec, list, t0, t1 | skip, progress)* must be created in a numerical code to make these detailed lists. For example, the numbers of suspended particles that enter the upper and lower settling tanks depending on the friction coefficient variable in the model taken for the constant channel bed slope must be calculated (Fig. 13). With the application of the HISTORY object in the SOLFEC

program, the exact position of certain suspended particles (or stone pebbles) in time can be obtained. The previously defined geometric position of the upper and lower settling tanks in the model (Fig. 15) did not represent a large problem for calculating the overall number of the particles that are deposited in them. Fig. 16 and 17 show the percentage of passing suspended particles (stone pebbles in this example) on the upper and lower settling tanks, depending on the time series for different friction coefficients (ranging from 0,0 ÷ 0,3 Pas).

The SOLFEC program provides a variety of other aspects of perception and analysis within the domain of open flow hydraulics (overflows, water jump, stresses on weirs, disseminates demersal and floating suspended material in the channel, flow around the bridge abutments, and so on).

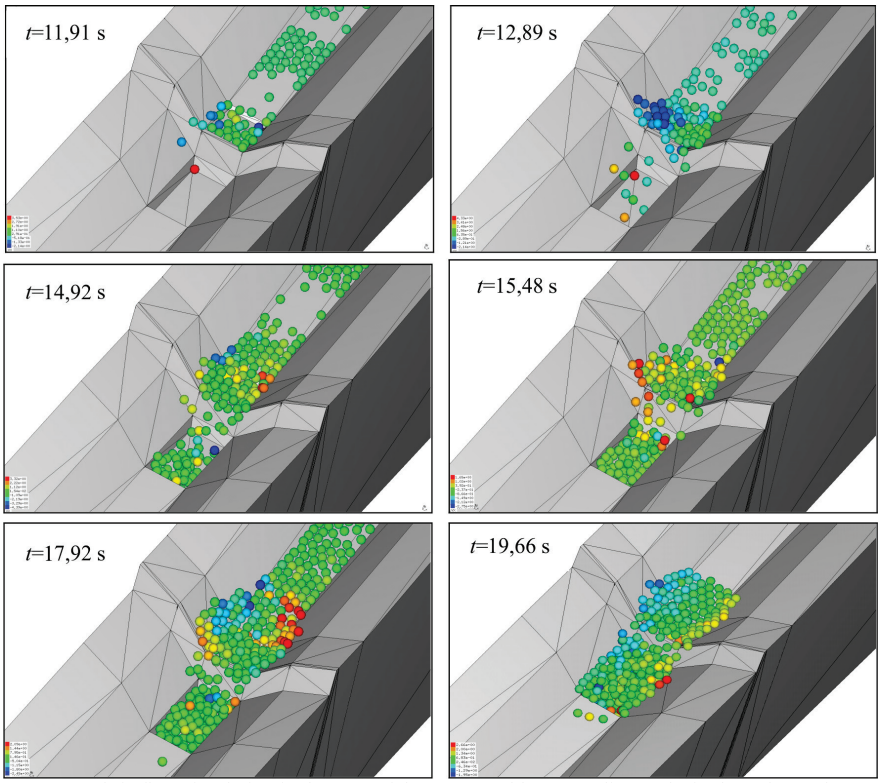

Figure 13 Debris flow simulation in the case of the upper and lower settling tanks in the Salt Creek stream

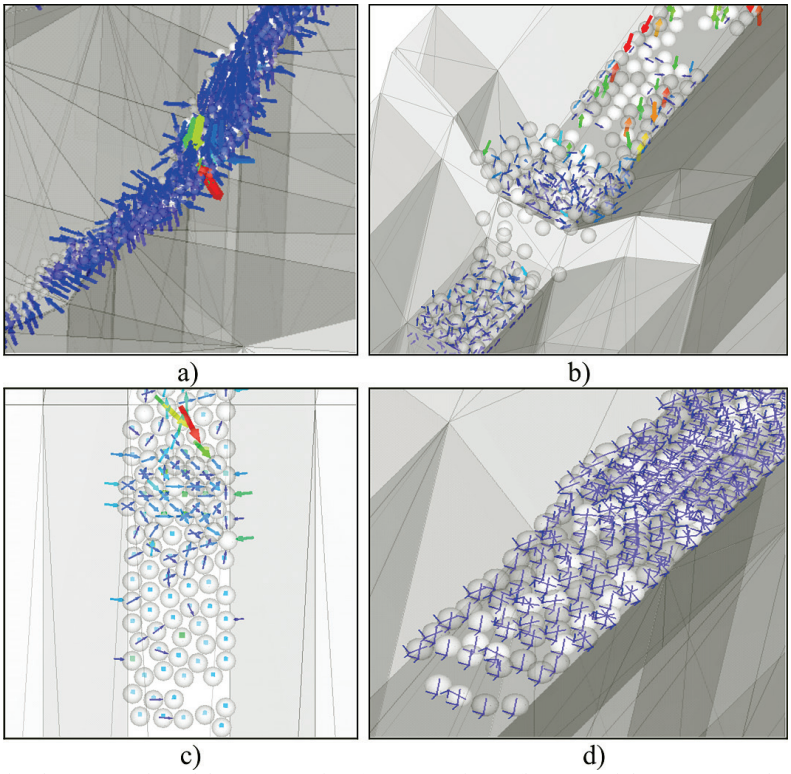

Figure 14 Visual representation of the contact points (a), contact forces (b), tangential stresses (c) and cutting forces (d) within the SOLFEC program

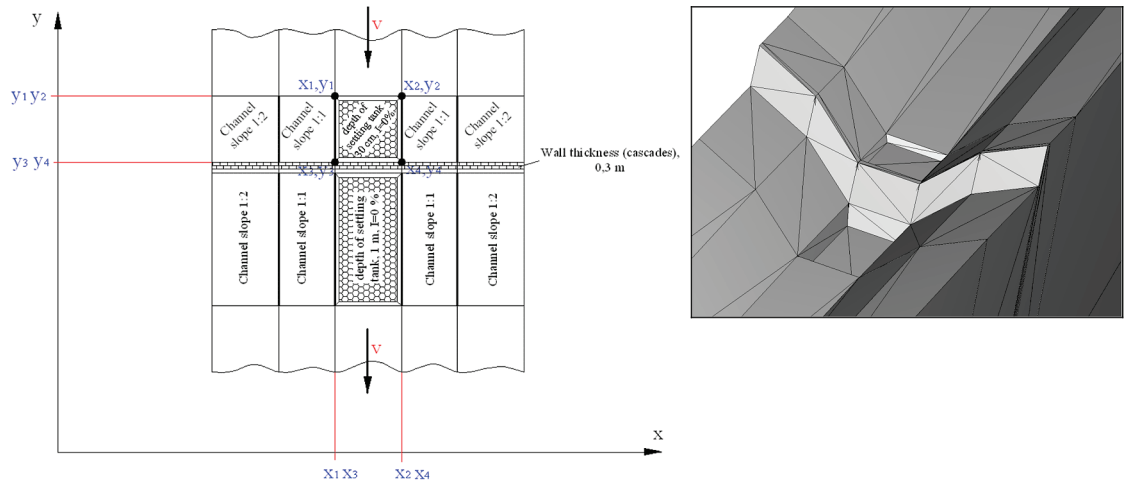

Figure 15 Graphical view of the upper and lower settling tanks within the Salt Creek stream

The total number of incoming particles / -	Time t / s	Friction coefficient / Pa·s	Diameter of particles / m	Number of particles in the upper settling tank / -	Time t_1 / s	The channel slope I / %	Time t_2 / s	Density of particles ρ / kg/m^3	Time increment Δt / s	Duration of calculation / s	Young's modulus / N/m^2	Poisson's coefficient / -
328	8,415	0,00	0,3	328	14,02	2,0	9,38	1800	0,005	100	15×10^9	0,25
328	10,33	0,10	0,3	296	20,22	2,0	12,04	1800	0,005	100	15×10^9	0,25
328	10,48	0,15	0,3	210	25,775	2,0	11,83	1800	0,005	100	15×10^9	0,25
328	10,56	0,20	0,3	155	25,1	2,0	11,17	1800	0,005	100	15×10^9	0,25
328	10,78	0,25	0,3	118	22,335	2,0	12,49	1800	0,005	100	15×10^9	0,25
328	10,83	0,30	0,3	74	22,825	2,0	12,83	1800	0,005	100	15×10^9	0,25

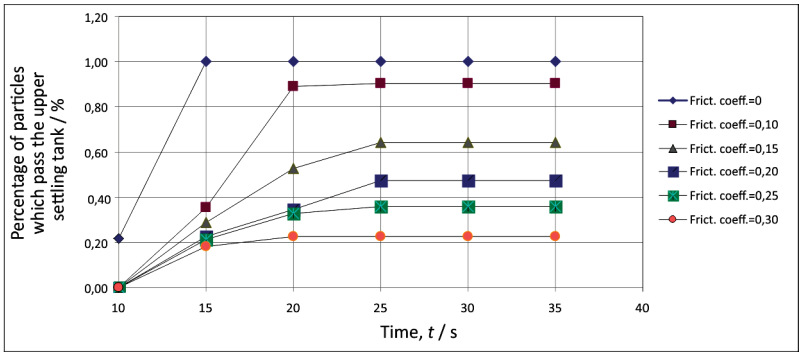

Figure 16 The percentage of passing suspended particles (stone pebbles) on the upper settling tank depending on the time and friction coefficient. Time t denotes time when first suspended particle entered in the upper settling tank, time t_1 represents elapsed time for collecting particles in the upper settling tank, time t_2 denotes the elapsed time to the first entry of particle into the lower settling tank.

The total number of incoming particles / -	Time t (t_2) / s	Friction coefficient / Pa·s	Diameter of particles / m	Number of particles in the lower settling tank / -	Time t_3 / s	The channel slope I / %	Time t_4 / s	Density of particles ρ / kg/m^3	Time increment Δt / s	Duration of calculation / s	Young's modulus / N/m^2	Poisson's coefficient / -
328	9,38	0,00	0,3	313	15,94	2,0	10,25	1800	0,005	100	15×10^9	0,25
328	12,04	0,10	0,3	219	22,24	2,0	14,995	1800	0,005	100	15×10^9	0,25
328	11,83	0,15	0,3	169	30,38	2,0	-	1800	0,005	100	15×10^9	0,25
328	11,165	0,20	0,3	104	25,3	2,0	-	1800	0,005	100	15×10^9	0,25
328	12,495	0,25	0,3	75	24,4	2,0	-	1800	0,005	100	15×10^9	0,25
328	12,825	0,30	0,3	64	24,205	2,0	-	1800	0,005	100	15×10^9	0,25

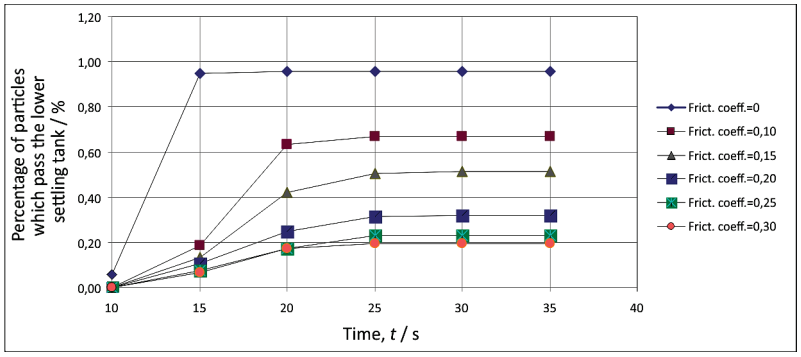

Figure 17 The percentage of passing suspended particles (stone pebbles) on the lower settling tank depending on the time and friction coefficient. Time t_2 denotes the elapsed time to the first entry of particle into the lower settling tank, time t_3 represents elapsed time for collecting particles in the lower settling tank, time t_4 represents the elapsed time until the release of the first particle from the lower settling tank.

4 Verification of the numerical model

Based on the hydraulic analysis carried out on the Salt Creek stream, the verification of numerical model of debris flow propagation was performed using SOLFEC program/code (the numerical model was verified with a coefficient of friction of 0,2 Pas). The hydraulic analysis was performed based on hydrological data on the rainfall intensity in a given area, specifically for the measured peak intensity of precipitation which occurred over a period from $1^{st} \div 2^{nd}$ November 2012 (total precipitation 82,6 mm, the maximum intensity of rainfall 16,2 mm/15 min). Based on previous measurements of the channel bed slope ($I_{channel}$ =1,67 %), the cross-section in front of the upper settling tank, depending on the water level in the channel (A-h), and adopted roughness coefficient for a given channel (n=0,04 $m^{-1/3}s$; taken value for channel that has coated with creeping dense grass and occasional bushes, previously roughened bottomed channel with occasional large pebbles, poorly maintained canals/torrents) the consumption curve was determined, i.e. the variation of flow in the channel Q (m^3/s) as a function of water level h (m), (Figs. 18 and 19, Tab. 1). The values of the water level during the conducted experiments were provided by a Mini Diver instrument (MD No.7) placed 2 m upstream from the start of the upper settling tank (the reason for this is the emergence of depression line in the channel, which may affect the accuracy of water flow calculation!), Fig. 19.

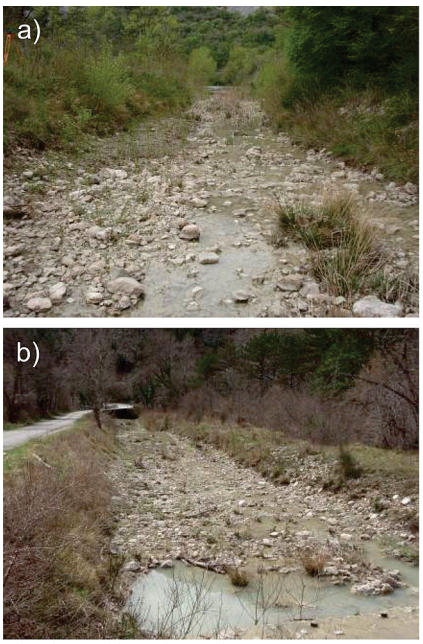

Figure 18 The view of the Salt Creek stream: a) upstream of the upper settling tank, b) downstream of the lower settling tank (Photo: Elvis Žic)

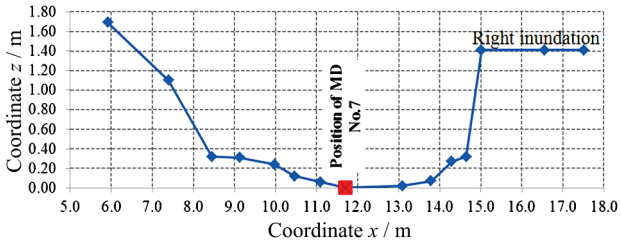

Figure 19 The Cross-section profile of Salt Creek stream, just upstream of the upper settling tank (measured on the position of MD No.7)

Table 1 The consumption (flow) curve on the cross-section inside the Salt Creek stream immediately upstream of the upper settling tank (position of MD No.7)

Height of channel, z / m	Area of cross-section, A / m^2	Surface width of channel, B / m	Wetted scope, O / m	Hydraulic radius, R / m	Manning roughness coefficient, n / $m^{-1/3}s$	Chezy coefficient, C / $m^{1/2}/s$	The slope of the bottom channel, I / -	Flow velocity, v / m/s	Water flow, Q / m^3/s
0,05	0,062	2,16	2,160	0,028	0,04	13,82	0,01677	0,302	0,019
0,10	0,197	3,05	3,065	0,064	0,04	15,82	0,01677	0,519	0,102
0,15	0,362	3,50	3,534	0,102	0,04	17,10	0,01677	0,709	0,257
0,20	0,546	3,85	3,906	0,140	0,04	18,01	0,01677	0,872	0,476
0,25	0,749	4,22	4,291	0,174	0,04	18,69	0,01677	1,011	0,756
0,30	0,972	4,82	4,903	0,198	0,04	19,09	0,01677	1,101	1,070
0,40	1,554	6,07	6,216	0,250	0,04	19,84	0,01677	1,285	1,996
0,50	2,179	6,30	6,520	0,334	0,04	20,83	0,01677	1,559	3,398
0,60	2,814	6,53	6,825	0,412	0,04	21,57	0,01677	1,794	5,047
0,70	3,478	6,76	7,129	0,488	0,04	22,18	0,01677	2,007	6,980
0,80	4,166	6,99	7,433	0,560	0,04	22,70	0,01677	2,201	9,167
0,90	4,876	7,22	7,737	0,630	0,04	23,15	0,01677	2,380	11,602
1,00	5,609	7,44	8,051	0,697	0,04	23,54	0,01677	2,544	14,269
1,10	6,752	7,83	8,544	0,790	0,04	24,04	0,01677	2,767	18,685
1,20	7,551	8,15	8,920	0,847	0,04	24,32	0,01677	2,897	21,876
1,30	8,382	8,47	9,297	0,902	0,04	24,57	0,01677	3,022	25,327
1,40	9,247	8,73	9,739	0,949	0,04	24,78	0,01677	3,128	28,920
1,50	10,140	9,12	10,040	1,010	0,04	25,04	0,01677	3,259	33,046
1,60	11,066	9,45	10,438	1,060	0,04	25,24	0,01677	3,366	37,250
1,70	11,981	11,13	12,168	0,985	0,04	24,94	0,01677	3,204	38,388

The consumption (flow) curve, along with input geometric and kinematic parameters, was used for the description of debris flow conducted in SOLFEC program, Fig. 20. The calculation for determining the applicable number of stone pebbles that pass upper and lower settling tanks inside the Salt Creek stream within the specified period of time was done by visual perception on the spot, using a high-speed frequency video camera, type Canon EOS Kiss X4. For added safety and control, three additional measurements were performed in the same time period in a way in which three people separately counted stone boulders which filled the upper

and lower settling tanks, Fig. 21. The total deviation of the measured data of three individual measurers obtained on the basis of average data calculated in counting the stone pebbles accounted for 13 % (for the first (upper)) and 9 % (for the second (lower)) settling tank compared to the measured values obtained with high-speed video camera. We took pebbles recorded with a high-speed video camera that allows slow motion video to the hundredth of a second as the measured value of passing stones. The analysis and calculation were performed using Adobe Photoshop CS6 64-bit software.

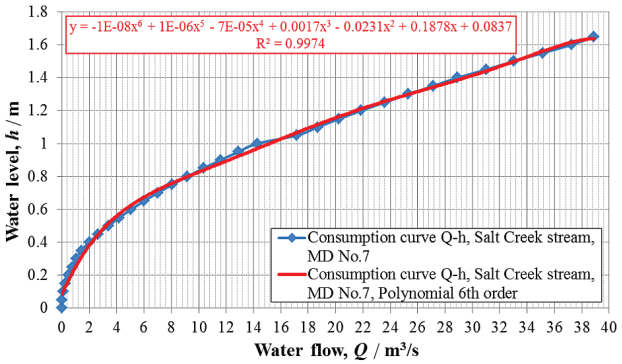

Figure 20 Consumption (flow) curve at the position of Mini Diver instrument (MD No.7), just above the upper settling tank, Salt Creek stream

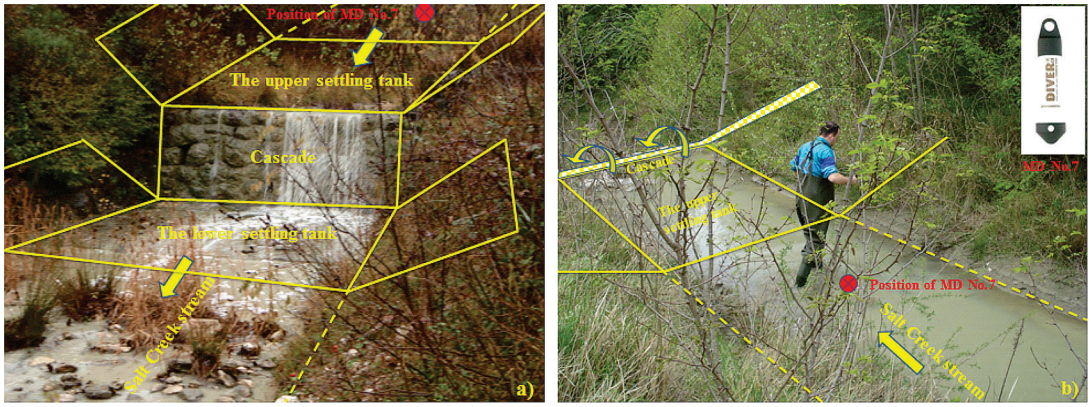

Figure 21 The measurement of the transience of stone pebbles on the Salt Creek stream: a) a view of disposition of the upper and lower settling tank, b) a view of disposition of Mini Diver instrument (MD No.7) upstream from the upper settling tank, (Photo: Elvis Žic)

Table 2 The verification of the numerical model developed in SOLFEC program. Comparison of calculated (SOLFEC program) and measured (terrain measurements) values of the number of transient stone pebbles (suspended particles) on the example of the upper and lower settling tank on the Salt Creek stream, Dubračina catchment area, Vinodol Valley

					Application of SOLFEC program		Terrain measurements		Percentage of deviation	
Diameter of particles / m	Density of particles, ρ / kg/m^3	Friction coefficient / Pa·s	The total number of incoming particles / -	Time t / s	Number of particles in the upper settling tank / -	Number of particles in the lower settling tank / -	Number of particles in the upper settling tank / -	Number of particles in the lower settling tank / -	The upper settling tank / %	The lower settling tank / %
0,3	1800	0,20	328	10.56	1	0	1	0	0.00	0.00
0,3	1800	0,20	328	11.00	36	7	33	5	9.09	40.00
0,3	1800	0,20	328	14.00	112	18	107	22	4.67	-18.18
0,3	1800	0,20	328	18.00	274	46	259	42	5.79	9.52
0,3	1800	0,20	328	22.00	183	83	190	77	-3.68	7.79
0,3	1800	0,20	328	25.10	155	102	148	105	4.73	-2.86
0,3	1800	0,20	328	25.30	155	104	148	106	4.73	-1.89

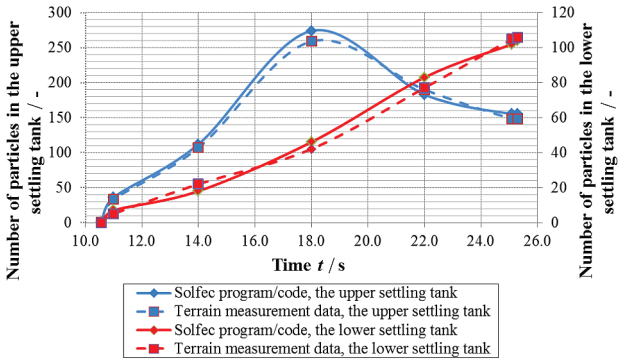

Figure 22 Graphical comparison of calculated (SOLFEC program) and measured (terrain measurements) values of the number of transient stone pebbles after a certain period of time

Tab. 2 and Fig. 22 show a comparison between the data obtained by the numerical model in SOLFEC program and the data measured on the Salt Creek stream, as well as the percentage deviation of given values after a certain period of time t. From the resulting comparisons we can conclude that the numerical model developed in SOLFEC program meets the description of debris flow propagation and filling of the upper and lower settling tank with stone pebbles very well, Tab. 2. The present numerical model in SOLFEC program can be used with success in other similar streams, torrents, rivers or artificially built (prismatic) channels. With this numerical model mudflow and pyroclastic "lahar" material propagation (the propagation of fine-grained materials) can also be observed, but at the same time carrying out a numerical simulation lasts much longer due to the high number of operations that are performed in SOLFEC

program (an extremely large number of fine-grained particles which are impinging and perform friction in contact with the bottom of channel). In this respect, the problems can be offset by using the cluster (super-computer), which also provides great storage output (calculated) data on a single hard drive.

5 Conclusion

The uncontrolled propagation of unbound rock material causes significant material and human losses. If the anticipated volume of unbound suspended matter, the range of distance, and the depth and speed of propagation can be estimated through mathematical modelling, significant losses could be avoided. Moreover, data from modelling can be used as input data in risk studies (geohazard analysis), which define hazardous work areas and appropriate protective measures. In recent decades, the phases of numerical flow modelling of unbound materials have been widely implemented within the framework of Continuum Mechanics (CM), so many new, sophisticated numerical models have been developed. Most of the available models are based on a heterogeneous and multi-phase mass movement as a single-phase continuum. If the shear resistance of the fluid phase is neglected, the stress tensor in the mixture can be decomposed into "pore-water pressure" and "effective stress". Then, the mechanical behaviour of mixtures can be described by the system of differential equations that governs the dynamics of each phase. After the initial and boundary conditions are identified, the spatial and temporal integration systems of differential equations can be carried out with numerical methods.

The SOLFEC program can be used to carry out simulation analyses of debris and mud flows, enabling more efficient and better estimates of input parameters that define the creation and launch of debris material in a particular area. The program also provides a quantified value for all input and output parameters that are necessary for the calibration and verification of numerical models. The main scientific contribution of the SOLFEC program is an extension of knowledge and understanding of the physical erosion processes on the rocky flysh complex, as well as a better understanding of the geohazard and propagation risk caused by unbound suspended rock material. The SOLFEC program can be used to assess geohazards and to determine safe and rational assessments of the appearance of debris and mud flows that are based on the critical geomorphological and hydrogeological parameters of the soil. The application of the SOLFEC program allows the phenomenon of unbound rock material propagation to be studied more precisely by implementing new erosional laws. The SOLFEC program is extremely important for establishing sustainable development in the wider research area of the Salt Creek stream. The implementation of simulation analyses will directly affect the spatial planning of the wider area and will allow a construction zone based on acceptable and unacceptable geohazards. The SOLFEC program may also allow guidelines to be created for future geozoning in flysch areas.

Acknowledgements

Research for this paper was conducted within the bilateral international Croatian-Japanese project "Risk identification and Land-Use Planning for Disaster Mitigation of Landslides and Floods in Croatia" and as a part of the scientific project "The Hydrology of sensitive water resources in karst" (114-0982709-2549) financed by the Ministry of Science, Education and Sports of the Republic of Croatia. This research was performed with financial support from the Japan International Cooperation Agency (JICA). Elvis Žic would like to thank the National Foundation for Science, Higher Education and Technological Development of the Republic of Croatia for the financial support during his research activities at the Faculty of Civil Engineering University of Glasgow (Scotland).

6 References

[1] Iverson, R. M. The physics of debris flows. // Review of Geophysics. 35, 3(1997), pp. 245-296.
[2] Blanc, T. Numerical simulation of debris flows with the 2D - SPH depth integrated model. Master thesis, 2008, 115 pages
[3] Debris flow and related phenomena // Entrainment of material by debris flows / Hungr, O.; McDougall, S.; Bovis, M. Praxis-Springer, Chapter 7, 2005. pp. 135-158.
[4] Coussot, P.; Meunier, M. Recognition, Classification and Mechanical description of debris flows. // Earth Sciences Reviews. 40, (1995), pp. 209-227.
[5] Rickenmann, D.; Zimmermann, M. The 1987 debris flows in Switzerland: documentation and analysis. // Geomorphology. 8, (1993), pp. 175-189.
[6] Davies, T. R.; Phillips, C. J.; Pearce, A. J.; Zhang, X. B. Debris flow behaviour - an integrated overview. // Erosion, debris flow and environment in mountain regions, Proceedings od Chengdu Symposium / IAHS Publication, No. 209, 1992.
[7] Wen, B. P.; Aydin, A. Mechanism of rainfall induced slide-debris flow: Constraints from its microstructure of its slip zone. // Engineering geology. 78, (2005), pp. 69-88.
[8] Takahashi, T. Debris flow: Mechanics, Prediction and Counter Measures. Taylor & Francis, Leiden, Netherlands, 2007.
[9] Rickenmann, D.; Chen, CL. Debris-flow hazards mitigation: mechanics, prediction, and assessment. Book of Proceedings of the Third international conference, Millpress, Davos, Switzerland, 2003.
[10] Rubinić, A. Hydrology of Dubračina catchment area. Faculty of Civil Engineering University of Rijeka, Graduate thesis, 2009, 71 pages.
[11] Benac, Č.; Jurak, V.; Ostrić, M.; Holjević, D.; Petrović, G. The phenomenon of excessive erosion in the area of Salt Creek stream (Vinodol valley). // Proceedings of the Third Croatian Geological Congress, Institute of Geological Research / Zagreb, 2005, pp. 173-174.
[12] Oštrić, M.; Horvat, B. Land Cover/Land Use Change Impact on Surface Runoff in Small Catchments. // The Third International Scientific Conference BALWOIS 2008, Ohrid, Republic of Macedonia, 2008, The Web version (2009), URL: http://www.conferencealerts.com/show-event?id=ca13336i (17.01.2010.).
[13] Benac, Č.; Dugonjić, S.; Arbanas, Ž.; Oštrić, M.; Jurak, V. The origine of instability phenomena along the karst-flysch contacts. // Proceedings of the regional symposium of the International Society for Rock Mechanics, Eurock 2009 / Taylor & Francis Group, Dubrovnik, 2009, pp. 757-762.

[14] Blašković, I. Tectonics of Part of the Vinodol Valley within the Model of the Continental Crust Subduction. // Geologia Croatica. 52, 2(1999), pp. 153-189.
[15] Ružić, I.; Sušanj, I.; Ožanić, N.; Žic, E. Salt Creek stream and Dubračina river spring runoff characteristics, Vinodol valley. // Proceedings of the Fifth Croatian Water Conference – Croatian waters facing the challenge of climate changes / Opatija, 2011, pp. 225-236.
[16] Gajski, D. Fundamentals of laser scanning from the air. // Ekscentar. 10, (2007), pp. 16-22.
[17] Štargel, K. Visualization of fluid dynamics simulation (gaseous fluid). Faculty of Electrical Engineering and Computer Science, University of Zagreb, Zagreb, Graduate thesis, 2006, 82 pages.
[18] Moreau, J. J. Numerical aspects of the sweeping process. // Computer Methods in Applied Mechanics and Engineering. 177, 3-4(1999), pp. 329-349.
[19] Jean, M. The non-smooth contact dynamics method. // Computer Methods in Applied Mechanics and Engineering. 177, 3-4(1999), pp. 235-257.
[20] Koziara, T. Aspects of computational contact dynamics. University of Glasgow, PhD thesis, Glasgow, 2008, 213 pages
[21] Koziara, T.; Bićanić, N. Smoothed variational inequality formulation of dynamic multibody frictional contact problems. // International Conference on Particle-Based Methods, Barcelona, 2009, The Web version (2009), URL: http://congress.cimne.com/particles2009/frontal/default.asp (18.07.2010.).
[22] Koziara, T.; Bićanić, N. Simple and efficient integration of rigid rotations suitable for constraint solvers. // Journal for Numerical Methods in Engineering. 81, 9(2009), pp. 1073-1092.
[23] Adams, M. F. A distributed memory unstructured Gauss-Seidel algorithm for multigrid smoothers. // Supercomputing 2001: Proceedings of the 2001 ACM/IEEE Conference on Supercomputing / ACM Press, New York, 2001, pp. 4-4.
[24] Žic, E.; Bićanić, N.; Koziara, T.; Ožanić, N. Numerical Modeling of suspended sediment propagation in small torrents. // Proceedings of the People, Buildings and Environment 2012 Conference / Lednice, Brno University of Technology, Faculty of Civil Engineering, 2012, pp. 661-670.
[25] Ožanić, N.; Sušanj, I.; Ružić, I.; Žic, E.; Dragičević, N. Monitoring and analyses for the working group II (WG2) in Rijeka area in Croatian-Japanese project. // 2nd Project Workshop, Monitoring and analyses for disaster mitigation of landslides, debris flow and floods, Book of proceedings / University of Rijeka, Rijeka, 2012, pp. 86-90.
[26] Žic, E.; Bićanić, N.; Koziara, T.; Ožanić, N.; Ružić, I. Application of the Solfec program for the Numerical Modeling of suspended sediment propagation in small torrents. // 2nd Project Workshop, Monitoring and analyses for disaster mitigation of landslides, debris flow and floods, Book of proceedings / University of Rijeka, Rijeka, 2012, pp. 98-101.

Authors' addresses

Elvis Žic, MSc. Assistant
Faculty of Civil Engineering
University of Rijeka
Radmile Matejčić 3, 51000 Rijeka, Croatia
E-mail: elvis.zic@uniri.hr

Nenad Bićanić, Full. Prof. Ph.D.
Faculty of Civil Engineering
University of Glasgow
School of Engineering
James Watt South Building, Glasgow G12 8QQ, Scotland
E-mail: bicanic@civil.gla.ac.uk

Lecturer Tomasz Koziara, Ph.D.
School of Engineering and Computing Sciences
Durham University
South Road, Durham, DH1 3LE, United Kingdom
E-mail: tomasz.koziara@durham.ac.uk

Nevenka Ožanić, Full. Prof. Ph.D.
Faculty of Civil Engineering
University of Rijeka
Radmile Matejčić 3, 51000 Rijeka, Croatia
E-mail: nozanic@uniri.hr